Journal of Engineering Science *Vol. XXVII, no. 4 (2020), pp. 80 - 87*
Fascicle *Electronics and Computer Science* *ISSN 2587-3474*
Topic *Electronics and Communication* *eISSN 2587-3482*

DOI: 10.5281/zenodo.4288280
CZU 004.942:620.9

DIGITAL TWIN FOR PV MODULE FAULT DETECTION

Sergey Valevich[1], ORCID ID: 0000-0001-9324-8790,
Roustam Asimov[2], ORCID ID: 0000-0002-4033-4238,
Ingmar Kruse[3], ORCID ID: 0000-0001-7074-6172,
Vitaly Asipovich[1]*, ORCID ID: 0000-0001-9658-2866

[1]*Belarusian State University of Informatics and Radioelectronics, Human Engineering and Ergonomics Department, P. Brovki, 6, Minsk, 220013, Republic of Belarus*
[2]*Sensotronica Ltd, Kulman, 9, 373, Minsk, 220010, Republic of Belarus*
[3]*SunSniffer GmbH & Co. KG, Ludwig-Feuerbach-Str. 69, Nuremberg 90489, Germany*
*Corresponding author: Vitaly Osipovich, *v.osipovich@bsuir.by*

Received: 09. 28. 2020
Accepted: 11. 23. 2020

Abstract. This paper is focused on photovoltaic (PV) installation fault detection techniques. Three methods of PV module fault detection were proposed, implemented, and tested on real PV plant located in Nürnberg, Germany. Proposed methods are based on calculation results produced using the Digital Twin (DT) concept. Power values at maximum power point (MPP) under standard test conditions are used during the calculations (as *Pmpp)*. *Pmpp* distributions by each month method is based on the statistical distribution of all PV modules from the same plant grouped by months, *global Pmpp distribution* method uses all available data uses similar approach with no month-related specifics, and *Pmpp average calculations* method is based on the average points calculation for each module during the period. All of these approaches provide entirely accurate results and allow finding modules with faults. However, the boundary abnormal modules count varies in each method, and additional module-based analysis may be required based on the purpose (monosemantic results for the most abnormal modules against more comprehensive results which include boundary modules).

Keywords: *Digital twin, photovoltaic, module degradation, module fault detection, fault detection.*

Introduction

In the PV field, regarding the importance of sustainability, monitoring systems are a paramount component for yield assessment. Nevertheless, in the industrial production, fault detection remains a manually handled issue [1, 2].

Most of the module faults are not stable over time and may affect the overall PV plant power generation in varying degrees. Problems may appear due to electrical issues, climate, location factors, soiling, shading, multiple connection issues, and others. Each type would affect the PV module's performance.

The long term reliability of photovoltaic modules is crucial to ensure the technical and economic viability of PV as a successful energy source. The analysis of degradation

mechanisms of PV modules is critical to ensure the current lifetimes exceeding 25 years. [3, 4, 5]

Faults are responsible for significant power loss, and sometimes, even dramatical damages are reported, such as fire hazard or material deterioration [1]. It is critical for PV plant's cost-effectiveness, primarily due to the long-time payback and long-term warranty period of typical PV modules.

Therefore, regular monitoring and high-quality maintenance are critical for any PV plant.

Various ways of monitoring and analysis include visual inspections, I–V curve field measurements, thermal evaluations by IR imaging, artificial intelligence techniques, and measurements of the I–V characteristics. [6, 7, 8] Electroluminescence technique is also used as a method for detecting defects in PV modules [9].

For customers, PV module characterization is essential to observe the output performance of their PV system and to proof intactness of single modules. For this purpose, reliable and nondestructive testing methods are desirable [10]. MPP parameters allow determining most of the defect types on different PV plant levels. Module-level faults may be found and analyzed using the telemetric data from the module's sensors over time. DT virtual laboratory [11] helps to calculate additional module parameters for more detailed defect analysis and extensive monitoring data [12]. For example, abnormal resistance levels may indicate electrical issues.

It must be noted that new defects that arise when the module is in operation may appear in modules initially defect-free (called hidden manufacturing defects) [9].

This paper is aimed at the detection of the individual PV module faults. Module arrays are usually built from similar module types, so with telemetric data from the sensors over time, each module could be analyzed and compared with other modules from this array in addition to the usual metrics. The main idea consists of two points. At first, all modules with defects need to be identified. Secondly, all abnormal boundary modules (which may have faults or not) should be separated from fault modules and partly analyzed.

Several approaches are presented based on a different distribution of apparent and boundary faults in modules: P_{mpp} distributions by each month, global P_{mpp} distribution, $P_{mpp\ avg}$ calculations with two diagram types for additional accuracy.

Methods of module efficiency analysis and fault detection

PV plant in Nürnberg, Germany, named Südstadt-Forum, is used for data aggregation and calculations in this paper. Plant includes three inverters (SUN2000-20KTL, Sinvert PVM17, and Sinvert PVM20 models) with 16 strings (PV module arrays) and 287 PV modules. Most of the strings consist of 18 PV monocrystalline modules – M190 (STORM Energy GmbH, Germany).

DT platform prepared API for module-by-module calculations based on input data. Input data includes the following parameters: voltage, current, temperature, irradiation from devices, temperature from devices, timestamp. These parameters are obtained by telemetry. During the experiment, all the data from June 2018 till November 2018 was used. Data was collected using Sunsniffer API.

The output contains the following params: power, voltage and current at MPP under standard test conditions (STC), series and parallel resistance, short circuit current and open-circuit voltage params.

On average, one new data point is acquired every 7 minutes. For example, Module 1.1_1 has 3943 points during August after all the filtering on the app side.

Most of the filtering stays inside DT calculation except some simple app-side preprocessing. Preprocessing excludes data points with missing parameters (empty temperature, current, voltage, timestamp values).

Aggregated results for individual modules are passed to the DT calculation API.

Three methods of statistical data analysis and defective modules search based on DT P_{mpp} calculations were implemented:

1) Power at MPP distributions by each month (P_{mpp} distributions by each month);
2) Global power at MPP distribution (global P_{mpp} distribution);
3) Average power at MPP calculations *(*$P_{mpp\ avg}$ calculations and two diagram types for additional accuracy).

Power at MPP distributions by each month

This method is based on the statistical distribution of all PV modules from the same plant. Similar PV cell models (at least by performance in the same module array) allow us to compare all modules and detect anything abnormal.

Statistical distribution with various module types and performance levels requires dynamic intervals for additional accuracy and better visibility.

Dynamic bin width for statistical P_{mpp} distribution was calculated in the following way using Min-Max value Eq.(1):

$$l_{P_{mpp}} = \frac{P_{mpp\,\max} - P_{mpp\,min}}{k}, \text{W} \quad (1)$$

Where k – bin number, calculated using Eq.(2):

$$k = \sqrt{n} \quad (2)$$

Where n – values count. k is an integer value (rounded up).

Diagrams of P_{mpp} statistical distribution using l_{Pmpp} as bin width by modules during 2018 by months are presented in Figure 1.

A) One outlier during June can be found in 124.27 – 129.92 W. Three more modules from range 163.82 – 169.47 W should be analyzed more. Additionally, one more outlier stays in 220.38 W and higher interval, which looks like an abnormal module, but not a defective one. Such a high P_{mpp} level across similar modules may be caused by a favorable module position (less shadowing effect, better angle, and others).

B) Two outliers during July can be found in 127.60 – 131.41 W interval. Three more modules from range 165.70 – 169.51 W should be analyzed more.

C) One outlier during August can be found in 134.21 – 137.65 W interval and also one more in 151.46 – 154.91 W. Two more modules from range 168.71 – 172.16 W should be analyzed more.

D) One outlier during September can be found in 143,25 – 146,08 W interval and also one more in 154.57 – 157.40 W. Four more modules from range 171.55 – 174.38 W should be analyzed more.

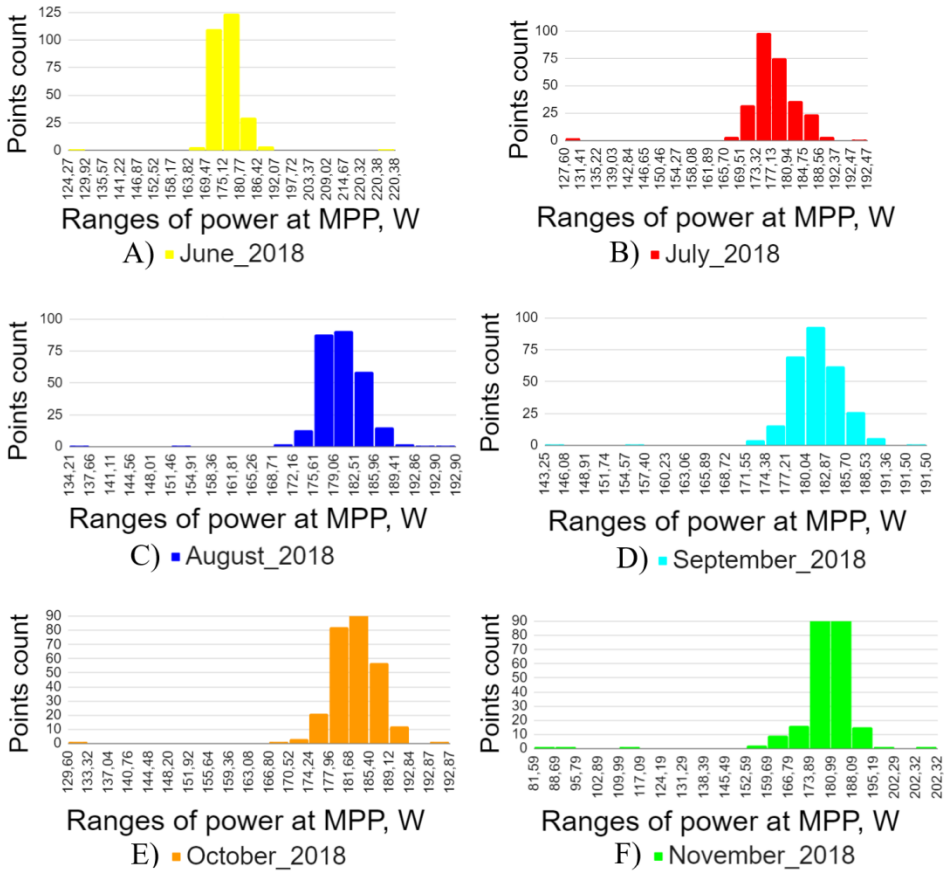

Figure 1. Distribution of P_{mpp} per modules during 2018.

E) One outlier during October can be found in 129.60 – 133.32 W interval. Also, four more modules should be analyzed more: 1 from range 166.80 – 170.52 W and three from range 170.52 – 174.24 W.

F) There're multiple outliers during November: one in 81.59 – 88.69 W interval, one in 88.69 – 95.79 W, one in 109.99 – 117.09 W intervals. Two modules from 152.59 – 159.59 W and nine modules from 159.59 – 166.79 W ranges also may be considered outliers and should be analyzed in a more detailed way.

Summary for outliers: June – 1 (+3 possible), July – 2 (+3 possible), August – 2 (+2 possible), September – 2 (+4 possible), October – 1 (+4 possible), November – 3 (+11 possible). Modules with outliers: 2.3_10 (June - 124.26 W, July - 127.59 W, August - 154.55 W, September - 143.24 W, October - 129.6 W, November - 115.14 W), 2.2_16 (July - 130.8 W, August - 134.2 W), 1.1_11 (September - 157.08 W), 1.11_15 (November - 81.59 W), 1.12_11 (November - 89.6 W). The total number of detected outliers for six months is 11 (+27 possible), five fault modules found.

Global power at MPP distribution

This method is similar to P_{mpp} distributions by each month. However, additionally, it includes all available data points (as much as possible). In our case – all the data from June 2018 till November 2018, 6 months in total) and may provide additional historical information about modules based on the period (e.g., module was normal during June – August period, and it became defective starting from September).

A combined diagram of P_{mpp} statistical distribution by modules during 2018 is presented in Figure 2.

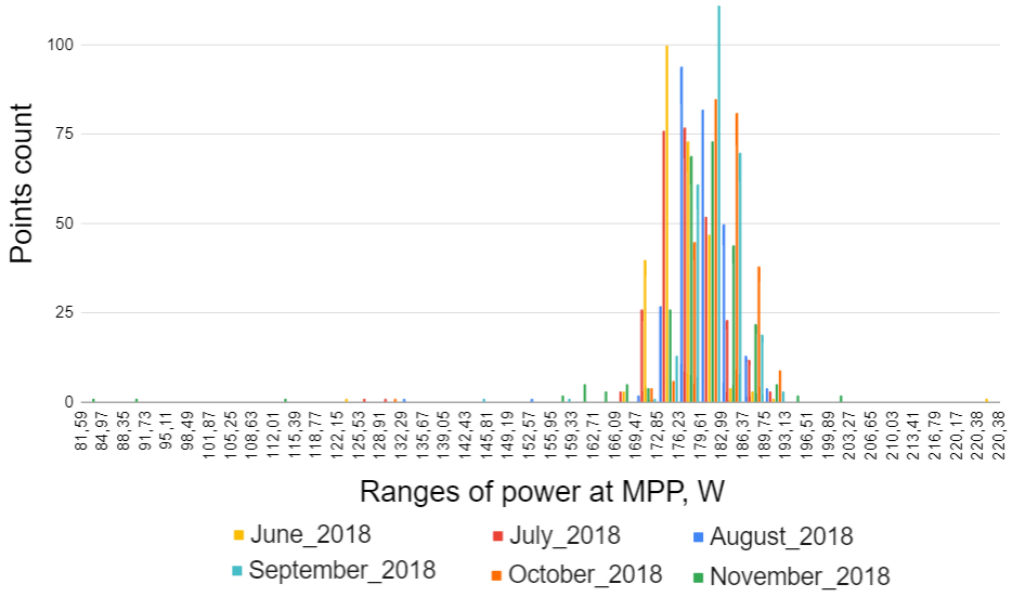

Figure 2. Global distribution of P_{mpp} per modules in June – November, 2018.

For this method, we use single and double distribution ranges. The most common double range is 176.23 – 182.99 W. All points from the left adjacent double range (169.47 – 176.23 W) are considered as valid too. Points from the next single range (166.09 – 169.47 W) should be analyzed more (possible outliers). Other points from the left side are considered as outliers.

Outliers from combined diagram: 1 in 81.59 – 84.97 W range, 1 in 88.35 – 91.73 W range, 1 in 112.01 – 115.39 W range, 1 in 122.15 – 125.53 W range, 1 in 125.53 – 128.91 W range, 1 in 128.91 – 132.29 W range, 1 in 132.29 – 132.67 W range, 1 in 142.43 – 145.81 W range, 1 in 152.57 – 155.95 W range, 3 in 155.95 – 159.33 W range, 5 in 159.33 – 162.71 W range, 3 in 162.09 – 166.09 W range.

11 additional points for more detailed analysis stay in 166.09 – 169.47 W range. Next range has 76 points and we consider it as normal P_{mpp} values.

Modules with outliers:

1) All modules from the previous method: 2.3_10 (June - 124.26 W, July - 127.59 W, August - 154.55 W, September - 143.24 W, October - 129.6 W, November - 115.14 W), 2.2_16 (July - 130.8 W, August - 134.2 W), 1.1_11 (September - 157.08 W), 1.11_15 (November - 81.59 W), 1.12_11 (November - 89.6 W).

2) Additional modules: 1.5_1 (November - 158.93 W), 1.5_11 (November - 158.72 W), 1.5_12 (November - 160.08 W), 1.5_3 (November - 161.54 W), 1.5_14 (November - 161.54 W), 1.5_13 (November - 162, 51 W), 1.5_17 (November - 162.32 W), 1.9_8 (November - 163.72 W), 1.5_9 (November - 163.76 W).

The total number of detected outliers for six months is 20 (+11 possible), 14 fault modules found.

Both ways of comparing provide quite a good view of defective modules. Nevertheless, single-month diagrams give an only clear understanding of modules with defects, whether the combined chart allows to separate all boundary values too (this next range above which contains 76 points while the previous range has only 11 points). Also, additional abnormal points and modules were found due to month specifics (November values look average in comparison with other November values in the previous method).

Average power at MPP calculations

The third method is based on the average points calculation for each module during the period. Then each module's deviation for each month allows us to find abnormal months for this specific module using its data from other months. Also, it shows unstable modules that vary a lot from month to month in performance.

Average P_{mpp} points are calculated for each module using the Eq.(3):

$$P_{mpp\ avg} = \frac{\sum_i^m P_{mpp}}{m} \quad (3)$$

Where m – number of months.

For the next analysis, average point difference percentage values were calculated using the Eq.(4):

$$P_{month\ \%} = \frac{P_{mpp} - P_{mpp\ avg}}{P_{mpp\ avg}} \quad (4)$$

$P_{mpp\ avg}$ calculations method of defective module detection is presented in Figure 3.

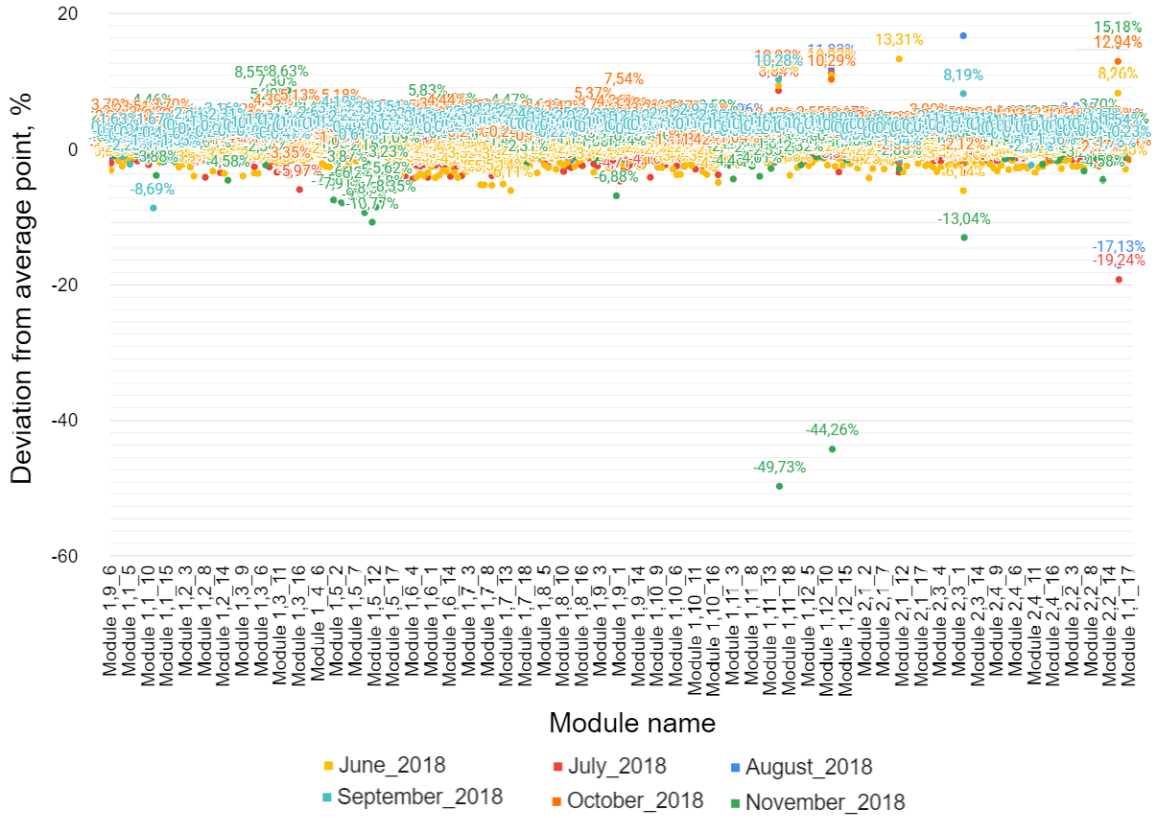

Figure 3. Average point distribution by deviation percentage.

This figure contains all $P_{month\ \%}$ values. In general, typical points should lie near 0% scale, both positive and negative values could be classified as outliers.

Module 2.2_16 has 5/5 outliers (one value is missing due to data issues for this specific month + module case). Module 2.3_10 has 3/6 outliers. Module 2.1_11 has 1/6 outliers. Module 1.12_11 has 5/5 outliers (one value is missing due to data issues for this specific month + module case). Module 1.11_15 has 6/6 outliers. Also, there are plenty of points for analyzing closer to the left diagram's part (especially in November).

An additional graph using only $P_{mpp\ avg}$ points was built to filter these boundary points and find fault modules. This graph is presented in Figure 4.

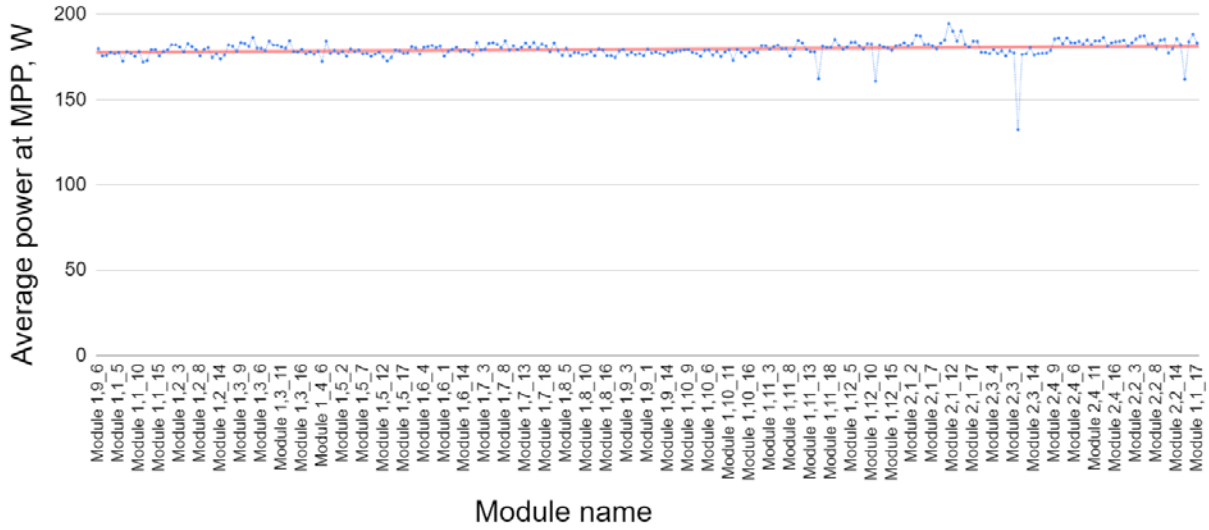

Figure 4. Average points of all modules.

All extremum values of this diagram represent the modules mentioned above: module 2.2_16, module 2.3_10, module 2.1_11, module 1.12_11, module 1.11_15. Furthermore, in comparison with the previous chart, there are no additional boundary values. Five points represent five modules, which are the most suitable modules for further analysis. Table 1 includes $P_{mpp\ avg}$ and $P_{month\ \%}$ values for two regular modules, and all detected defective modules (yellow values) for comparison.

Table 1

$P_{mpp\ avg}$ values and deviations per month

	$P_{mpp\ avg}$	June	July	August	September	October	November
Module 1,11_5	181.95	-2.02%	-1.20%	0.73%	0.48%	1.42%	0.58%
Module 1,12_3	179.6	-1.76%	-0.22%	1.01%	1.12%	2.16%	-2.32%
Module 1,11_15	162.31	9.36%	8.64%	10.52%	10.28%	10.93%	-49.73%
Module 1,12_11	160.78	10.93%	11.22%	11.83%		10.29%	-44.26%
Module 2,1_11	194.5	13.31%	-3.53%	-3.33%	-1.54%	-2.05%	-2.86%
Module 2,2_16	161.96	8.26%	-19.24%	-17.13%		12.94%	15.18%
Module 2,3_10	132.4	-6.14%	-3.63%	16.73%	8.19%	-2.12%	-13.04%

This combined table with the data from both Figures above allows finding modules with faults. Additionally, most of the points lay in the same range with small fluctuations in range (-5%; 5%). Some points outside this range should be analyzed more: 25 points below (<-5%) and 24 points above (>5%) from Figure 3. These values include points from the Table 1, so 25 - 6=19 points below, 24 - 15=9 points above, 19 + 9 = 28 possible outliers.

The total number of detected outliers for six months is 21 (+28 possible), five fault modules found.

Conclusions

P_{mpp} distributions by each month allows us to find the most abnormal modules.

Global P_{mpp} distribution allows the same as P_{mpp} distributions by each month and an additional clear border between points, which could be additionally analyzed.

$P_{mpp\ avg}$ calculations with two diagram types provide results from both the above methods (diagram with the most abnormal modules and chart with all additional boundary modules).

Thus three methods of module efficiency analysis are proposed based on P_{mpp} calculation results using physical and mathematical models from DT [11, 12].

All proposed methods could be used during the PV plant's operability monitoring.

References

1. Sarikh S., Raoufi M., Bennouna A., Benlarabi A. and Ikken B. "Fault diagnosis in a photovoltaic system through I-V characteristics analysis," 2018 *9th International Renewable Energy Congress (IREC)*, Hammamet, 2018, pp. 1-6, doi: 10.1109/IREC.2018.8362572.
2. Chen, Zhi-Cong & Wu, Lijun & Cheng, Shuying & Lin, Peijie & Wu, Yue & Lin, Wencheng. (2017). Intelligent fault diagnosis of photovoltaic arrays based on optimized kernel extreme learning machine and I-V characteristics. *Applied Energy*. 204. 10.1016/j.apenergy.2017.05.034.
3. Sánchez Friera, P., Piliougine, M., Peláez, J., Carretero, J. and Sidrach de Cardona, M. (2011), Analysis of degradation mechanisms of crystalline silicon PV modules after 12 years of operation in Southern Europe *// Progress in Photovoltaics: Research and Applications*, 19: 658-666.
4. Karim I. A. "Fault analysis and detection techniques of solar cells and PV modules", 2015 *International Conference on Electrical Engineering and Information Communication Technology (ICEEICT)*, Dhaka, 2015, pp. 1-4.
5. Fadhel S., Delpha C., Diallo D., Bahri I., Migan A., Trabelsi M., Mimouni M.F. PV shading fault detection and classification based on I-V curve using principal component analysis: Application to isolated PV system. *Solar Energy*, Volume 179, 2019, Pages 1-10, ISSN 0038-092X
6. Prashant Rajak, Dr. S.K. Bharadwaj, Dr. Suresh Kumar Gawre. PV Module fault detection & diagnosis. *International Research Journal of Engineering and Technology (IRJET)*, Volume 5, 2018, pp. 3809-3813
7. Mohamed Hassan Ali, Abdelhamid Rabhi, Ahmed El Hajjaji, Giuseppe M. Tina. Real Time Fault Detection in Photovoltaic Systems *// Energy Procedia*, Volume 111, 2017, Pages 914-923
8. Sayed A. Zaki, Honglu Zhu, Jianxi Yao. Fault detection and diagnosis of photovoltaic system using fuzzy logic control. *2019 4th International Conference on Sustainable and Renewable Energy Engineering (ICSREE 2019)*, article 02001 (2019), pp. 1-6
9. Munoz M., M. A. Alonso-Garcia, Nieves Vela, F. Chenlo. Early degradation of silicon PV modules and guaranty conditions. *Solar Energy*, Volume 85, Issue 9, September 2011, Pages 2264-2274
10. Sander M., B. Henke, S. Schweizer, M. Ebert and J. Bagdahn, "PV module defect detection by combination of mechanical and electrical analysis methods." *2010 35th IEEE Photovoltaic Specialists Conference*, Honolulu, HI, 2010, pp. 1765-1769.
11. Asimov R.M., Valevich S.V., Kruse I., Asipovich V.S. Virtual laboratory for testing of solar power plants in big data analysis. *Collection of materials of the V International Scientific and Practical Conference «BIG DATA and ADVANCED ANALYTICS»*, March 13–14, 2019, Minsk, BSUIR, pp. 61–65.
12. Osipovich V.S., Asimov R.M., Chernoshey S.V. Digital twin in the Analysis of a Big Data. *Collection of materials of the IV International Scientific and Practical Conference «BIG DATA and ADVANCED ANALYTICS»*, May 3–4, 2018, Minsk, BSUIR, pp. 69–78.